Sustainable Marine Structures
https://journals.nasspublishing.com/sms

ARTICLE

Monitoring Shoreline Evolution on Morocco's Northern Atlantic Coast Using Remote Sensing and DSAS

Hatim Haddaoui [1*] **, *Abdelhaq Aangri*** [2] **, *Smail Souiri*** [1] **, *Mounir Hakkou*** [1]

[1] *Earth Sciences Department, Scientific Institute of Rabat, Mohammed V University, Rabat 10000, Morocco*

[2] *Earth Sciences Department, Faculty of Sciences of Kenitra, Ibn Tofail University, Kénitra 14000, Morocco*

ABSTRACT

Coastal zones are dynamic interfaces responding to complex natural processes and anthropogenic pressures. Monitoring shoreline evolution is essential for sustainable coastal management, particularly given climate change, urban expansion, and sediment flux disruption. This study investigates shoreline changes along Morocco's northern Atlantic coast from 1990 to 2023, an area of strategic economic importance and environmental vulnerability. Landsat satellite imagery and geospatial techniques, including the Digital Shoreline Analysis System (DSAS v5.1) and the Normalized Difference Water Index (NDWI), provided a high-resolution, diachronic assessment. Shoreline extraction and image enhancement were conducted with ENVI software, and change detection utilized Linear Regression Rate (LRR) and End Point Rate (EPR) indicators. Results revealed significant spatial variability: sectors like northern Moulay Bousselham and Chlihat showed pronounced accretion (+3.2 to +4.7 m/year), while areas such as Tahaddart and southern Mehdia experienced severe erosion (up to −3.4 m/year). The total net eroded area exceeds 58,000 m^2. Trends correlate strongly with hydrodynamic forces, upstream damming, sediment extraction, and extreme weather events, notably storms in 2014 and 2017. Findings align with studies highlighting compounded effects of sediment starvation and sea-level rise. By integrating remote sensing, time-series analysis, and uncertainty quantification, this research provides insights into the primary drivers of shoreline dynamics, emphasizing the urgent need for adaptive, evidence-based coastal management strategies, including regulation of sand mining, sediment buffer restoration, and soft-engineering solutions.

Keywords: Shoreline Evolution; Erosion; Accretion; DSAS; ENVI

*CORRESPONDING AUTHOR:
Hatim Haddaoui, Earth Sciences Department, Scientific Institute of Rabat, Mohammed V University, Rabat 10000, Morocco; Email: hatim_haddaoui@um5.ac.ma

ARTICLE INFO
Received: 13 May 2025 | Revised: 12 June 2025 | Accepted: 3 July 2025 | Published Online: 31 July 2025
DOI: https://doi.org/10.36956/sms.v7i3.2146

CITATION
Haddaoui, H., Aangri, A., Souiri, S., et al., 2025. Monitoring Shoreline Evolution on Morocco's Northern Atlantic Coast Using Remote Sensing and DSAS. Sustainable Marine Structures. 7(3): 101–116. DOI: https://doi.org/10.36956/sms.v7i3.2146

1. Introduction

Coastal areas are dynamic environments influenced by both natural and anthropogenic processes that shape their evolution across various temporal and spatial scales [1,2]. Coastal erosion and accretion are major phenomena continuously modifying the shoreline, impacting ecosystems, infrastructure, and coastal populations [3–5]. In the context of climate change and increasing urbanization, analyzing historical shoreline trends is essential to understanding the mechanisms driving coastal evolution and anticipating associated risks [6,7].

The northern Atlantic coast of Morocco represents a strategic zone due to its economic importance and its vulnerability to erosion and marine submersion processes [8]. This region is subjected to multiple influences, including hydro-sedimentary dynamics, sea-level rise, and the impact of coastal infrastructure and dams that reduce fluvial sediment supply [9,10].

Within this framework, the present study proposes a long-term and zone-specific analysis of shoreline evolution between 1990 and 2023, relying exclusively on Landsat satellite imagery and the Digital Shoreline Analysis System (DSAS v5.1). The shoreline extraction is based on the Normalized Difference Water Index (NDWI), enabling precise diachronic mapping of coastal changes despite the limited spatial resolution of Landsat data [11,12].

The adopted methodology primarily uses multispectral images from the Landsat 5, 7, and 8 missions, selected for their availability and temporal consistency, which are critical for a diachronic study spanning over three decades. To enhance spatial accuracy in shoreline delineation, rigorous radiometric and geometric corrections were applied, along with a Brovey transform-based image fusion technique, improving the definition of coastal contours [12,13]. Satellite image processing and pre-treatment were conducted using ENVI software, which offers advanced tools for spectral index calculation, image enhancement, and classification.

Unlike other studies recommending field validation through topographic surveys or differential GPS measurements, this work relies solely on the advanced processing of Landsat imagery, due to the lack of recent ground truth data in the study area. This approach ensures a reliable and reproducible monitoring of shoreline changes over the analyzed period, while acknowledging limitations related to the 30-meter spatial resolution of the images [14–16].

The analysis also integrates robust statistical methods implemented in DSAS, including Linear Regression Rate (LRR) and End Point Rate (EPR) indicators, which quantify rates of shoreline erosion and accretion at various spatial and temporal scales. These indicators allow for an objective evaluation of coastal dynamics and the identification of zones undergoing significant change [1,17].

The expected outcomes of this research are (i) to delineate areas experiencing erosion and accretion, (ii) to determine shoreline change rates, and (iii) to provide a scientific basis to guide integrated coastal zone management strategies along the Moroccan northern Atlantic coast.

2. Materials and Methods

2.1.Study Area

The designated study area extends approximately 340 kilometers along the Atlantic facade of Morocco, spanning from the Tangier region at the northern coordinate (35°48′02″N, 5°54′22″W) to the southern limit in Rabat-Skhirat at “34°00’00’’ N, 06°57’00’’ W” (**Figure 1**).

This coastal stretch encompasses two crucial administrative regions, Tangier-Tetouan-Al Hoceima and Rabat-Salé-Kenitra, which include the provinces of Tangier-Assilah, Larache, Kenitra, Salé, Rabat, and Skhirate-Témara. Economically and strategically significant, these areas serve as major hubs of Moroccan development, with Tangier acting as a key industrial and logistic center, particularly through the Tangier-Med port, and Rabat functioning as the nation’s political capital.

The coastline within the study area exhibits a diverse range of coastal geomorphologies (**Figure 2**), including sandy beaches, rocky cliffs, and dunes. Specifically, dune formations account for 5% of the study area’s coastal environment, while rapidly receding sandy cliffs constitute 38%, sandy beaches cover approx-

imately 55%, and rocky cliffs make up 2% (**Figure 1**). From a granulometric perspective, this area is dominated by medium sand grains; Beach sediments are primarily composed of medium to fine quartz sand, with grain size and carbonate content varying according to local hydrodynamic conditions and sediment supply. The beaches are dynamically shaped by a combination of wave action, tidal influences, and fluvial sediment contributions, particularly from major rivers such as the Sebou and Loukkos.

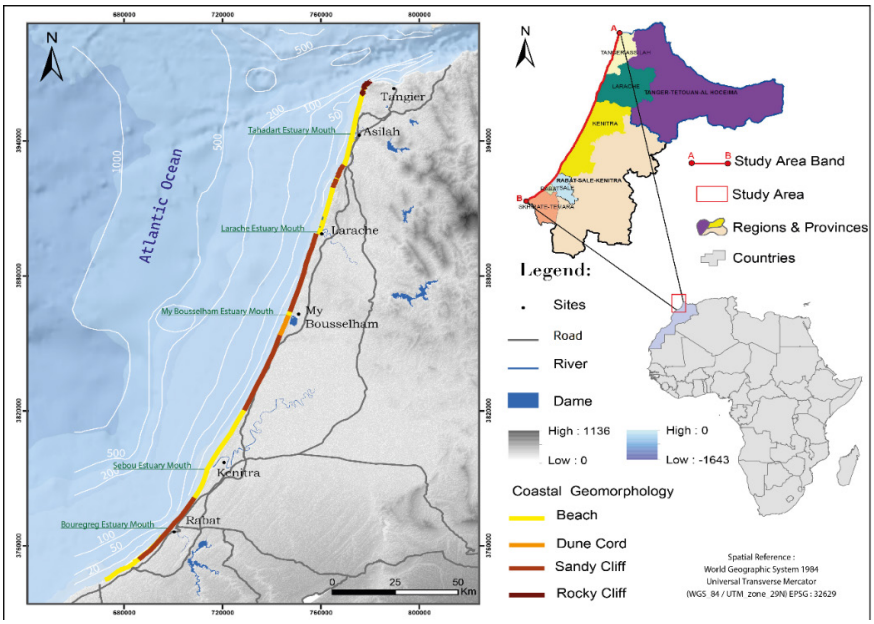

Figure 1. Geographic location and geomorphology of the study.

Figure 2. Examples of coastal sites studied.

This littoral is home to several ecologically sensitive zones, including estuaries and lagoons that serve as biodiversity hotspots (**Figure 1**). The Moulay Bousselham estuary, for example, is a Ramsar-listed wetland of international importance, supporting a diverse array of avian and marine species. These coastal systems are increasingly threatened by anthropogenic pressures, such as urbanization, industrialization, and coastal infrastructure development, which exacerbate erosion and disrupt sediment transport mechanisms [18].

Hydrodynamically, the northern Atlantic coast of Morocco is exposed to high-energy waves traveling roughly from the NW sector, which is generated by W–E tracking subpolar, deep, low-pressure systems over the North Atlantic Ocean and are therefore strongly seasonally modulated. Substantially higher waves are observed during the December, March winter period. The significant wave heights can exceed 8m during severe storms [19].

Between 1990 and 2023, the Study Area region experienced a Mediterranean climate characterized by warm, dry summers and mild, wet winters (**Figure 3**). Average temperatures typically increased from January's cool 12.5°C to a peak of around 26°C in August, then decreased towards December. Precipitation was most abundant in winter, peaking in November with about 120 mm, while the summer months were notably dry, especially in July and August, with almost negligible rainfall. Wind and wave patterns in the area generally followed seasonal trends, with stronger, more frequent winds in winter, and relatively calm conditions in summer (**Figure 3**).

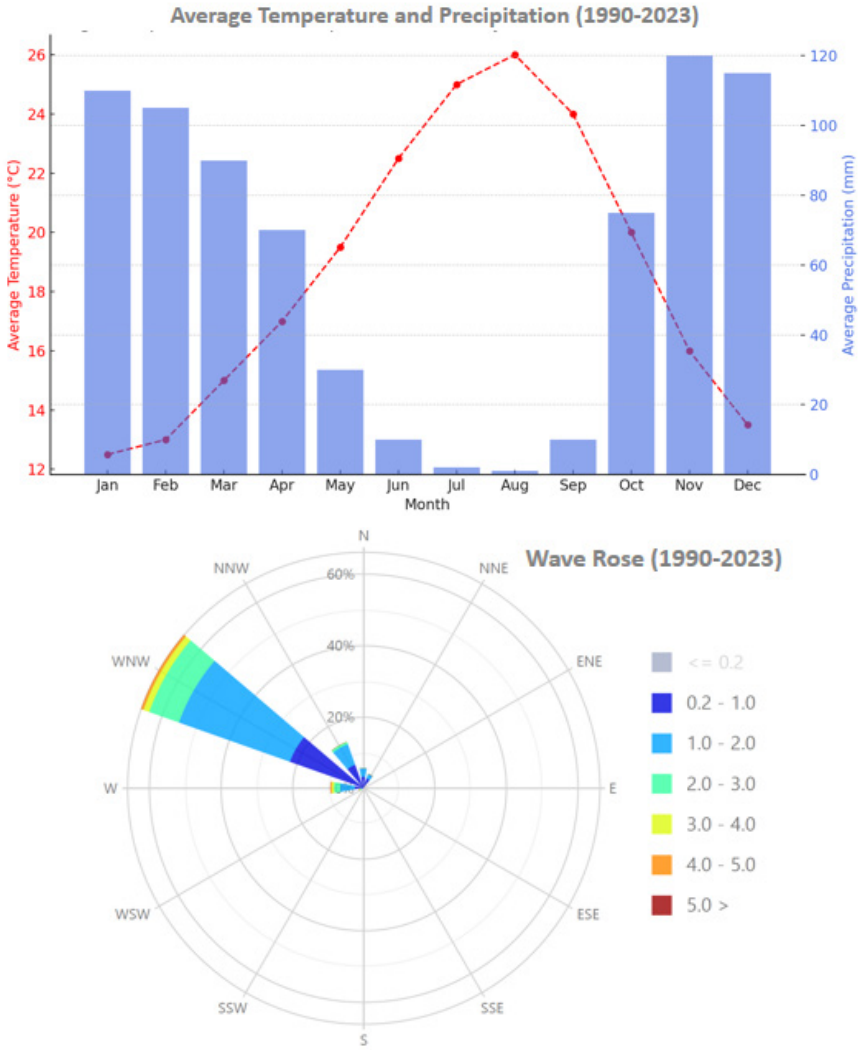

Figure 3. Climatic data of the study area.

2.2.Methodology

This study implemented a multi-step geospatial methodology to quantify shoreline evolution along the study area using satellite data from Landsat missions. Four reference years were selected: 1990, 2003, 2013, and 2023, forming a temporal series spanning over three decades (**Table 1**). These dates were chosen based on the availability of images with minimal cloud cover and seasonal comparability (preferably during summer months), in order to minimize the influence of temporary hydrodynamic variations (such as wave activity, tides, and river inflows).

Table 1. Characteristics of the Landsat imagery used in this research.

Acquisition Date/Time	Spacecraft ID/ Sensor	Path/Row	Pixel Size (m)	Coordinate System/Datum	Tide Height (m)
10/08/1990 – 14:10:32	Landsat 5/TM	202/036	30	UTM/WGS 84	2.87
17/07/2003 – 14:03:14	Landsat 7/ETM+	202/036	30	UTM/WGS 84	2.54
17/07/2013 – 11:06:14	Landsat 8/OLI_TIRS	202/036	30	UTM/WGS 84	2.60
17/07/2023 – 12:08:44	Landsat 8/OLI_TIRS	202/036	30	UTM/WGS 84	2.80

2.2.1. Satellite Image Preprocessing

The preprocessing of satellite imagery was a crucial step to ensure the spatial and radiometric consistency required for diachronic shoreline analysis. This step was conducted using ENVI 5.6, a remote sensing software widely used for the processing of Earth observation data. The workflow consisted of the following sequential operations:

a. Radiometric Correction

Radiometric correction was applied to all Landsat images (TM, ETM+, and OLI) to convert raw digital numbers (DNs) into physical reflectance values. This process minimized the influence of acquisition parameters such as sensor calibration differences, solar angle, and atmospheric scattering. It ensured that the reflectance values were comparable across all dates, allowing for consistent extraction of spectral indices like NDWI. In ENVI, this was achieved using the Radiometric Calibration tool, followed by Top-of-Atmosphere (TOA) Reflectance conversion, which accounts for solar elevation and Earth-Sun distance.

b. Geometric Correction

A geometric correction was carried out to ensure spatial alignment between images from different years. Using ground control points (GCPs) and a first-order polynomial transformation, each image was georeferenced to a common base image with a Root Mean Square Error (RMSE) less than 0.5 pixels. This precision level is essential for detecting shoreline shifts over time. The corrected images were then projected to the UTM Zone 29N coordinate system (WGS84 datum) to maintain consistency throughout the dataset.

c. Pan-sharpening (Spatial Enhancement)

To improve the visual quality and accuracy of shoreline detection, a pan-sharpening technique was applied using the Brovey transform. This method integrates the high-resolution panchromatic band with multispectral bands to produce sharpened images with enhanced spatial resolution (from 30 m to 15 m for Landsat ETM+ and OLI). This enhancement is especially valuable in complex coastal zones where small morphological features must be detected.

d. NDWI Calculation for Water-Land Separation

After preprocessing, the Normalized Difference Water Index (NDWI) was computed for each image to distinguish between water bodies and terrestrial surfaces. The NDWI is particularly effective on sandy coasts and is computed using the formula:

$$\mathrm{NDWI} = \frac{(\mathrm{Green} - \mathrm{NIR})}{(\mathrm{Green} + \mathrm{NIR})} \quad (1)$$

This index accentuates water features by taking advantage of the strong absorption of near-infrared radiation by water and its high reflectance in the green band. The NDWI images served as the base layer for shoreline digitization.

e. Visual Inspection and Manual Shoreline Digitization

While NDWI offers a robust automated approach, final shoreline extraction required manual digitization to correct for any misclassification due to cloud shadows, foam lines, or mixed pixels in turbid water zones. This step was carried out visually by overlaying NDWI on the sharpened multispectral composite and using expert interpretation to trace the High-Water Line (HWL) with high confidence.

2.2.2. Shoreline Extraction

The mapped coastlines derived from satellite data facilitated the identification of long-term processes spanning 33 years. A segmented analysis was conducted from 1990 to 2023 using the DSAS extension of ArcMap [20]. The DSAS tool is a Geographic Information System (GIS) tool that facilitates the creation of equidistant transects from a baseline [20]. These transects intersect the different shorelines, enabling the estimation of statistics such as the net movement of the coastline in meters. the End Point Rate (EPR) and The Linear Regression Rate in meters per year (LRR) was chosen from all the statistical parameters accessible within DSAS, as is commonly employed in shoreline investigations. The LRR ascertains a rate-of-change metric by fitting a least square regression to all shorelines at a specific transect. The LRR rates are determined by a best-fit regression line through the sample and possess the advantages that: (1) it employs a minimum of three data points to generate any outcome [20], (2) all of the data is employed regardless of the trend and precision of the data, (3) it is highly comprehensible and utilitarian. The changes in cross-shore distance (erosion or accretion) were quantified by examining sequences of transects with a separation of 100 meters.

2.2.3. Shoreline Change Computation

Shoreline change rates and distance between shorelines were calculated in this study by using two methods of the DSAS tools, which are EPR and LRR, transects were cast perpendicular to the baseline at regular 100 m intervals, spanning the entire coastline. The interaction between these transects and the shoreline at the baseline is leveraged to derive the statistical measures of the rate of change. The method employed for estimating the shoreline change rate in this research is the Linear Regression Rate (LRR) technique. The LRR algorithm utilizes the entirety of the available data to determine a line that minimizes the squared distances to the reference shoreline, which is a well-recognized approach for computing the enduring rates of shoreline alteration [21–24].

Additionally, the End Point Rate (EPR) was also computed for the shoreline using the same transects as the LRR. EPR is calculated by dividing the total shoreline movement distance by the time that has passed between the earliest and latest measurements at each transect.

2.2.4. Justification for the Choice of Shoreline Indicator

The shoreline was delineated using the High-Water Line (HWL), a proxy visually identifiable on optical satellite imagery due to the spectral contrast between wet and dry zones. Although several alternative shoreline indicators are well documented in the literature such as the vegetation line, dune base, or berm crest these could not be applied consistently across the study area or throughout the 33-year observation period. In many coastal zones, particularly sandy or urbanized environments, the HWL often represents the only feasible indicator due to the absence of stable vegetative cover, the dynamic nature of dune systems, or limited image resolution. This was the case in the present study area, where no other geomorphic markers were discernible with confidence across the entire dataset.

Despite its susceptibility to short-term hydrodynamic variability (e.g., tides, wave run-up), the HWL remains one of the most commonly used shoreline indicators worldwide, especially in long-term studies based on medium-resolution satellite imagery such as Landsat [25,26]. Its broad acceptance, ease of identification, and global comparability make it a pragmatic and reproducible choice for diachronic shoreline change analysis. However, it is important to acknowledge that using the HWL may introduce non-negligible uncertainties, especially when comparing shorelines extracted under different tidal or wave conditions. These limitations were mitigated in this study by selecting images from

seasonally similar periods, favoring summer acquisitions when shoreline positions tend to be more stable.

2.2.5. Error Analysis (Quantification of Shoreline Position Uncertainty)

In order to ensure the reliability of shoreline change rates calculated using the Digital Shoreline Analysis System (DSAS), the total uncertainty associated with shoreline positioning was assessed (**Table 2**). This uncertainty originates from several factors, including data acquisition conditions, image resolution, and the shoreline proxy used. Based on approaches proposed by Fletcher [27], two main categories of error were considered: positional uncertainty (e.g., due to tides and seasonal variations) and measurement-related uncertainty (e.g., digitizing, pixel size, and georeferencing).

Table 2. Uncertainties associated with shorelines obtained from different sources.

Error Type	Symbol	Estimated Value (m)	Remarks
Seasonal error	E_s	0	Neglected – all images acquired during summer
Tidal fluctuation error	E_t	5.0	Max tidal variation of 0.35 m; assumed gentle beach slope
Digitizing error	E_d	7.5	Half of Landsat pixel (30 m)
Pixel error	E_p	0	Included in digitizing error
Rectification error	E_r	7.5	Standard geometric error in Landsat Level-2 products
Total uncertainty	U_t	±11.72 m	Computed as root sum of squares of individual errors
Annualized uncertainty	U_a	±0.36 m/year	Over a 33-year period

1) Tidal Fluctuation Error (E_t): Tidal influence can lead to horizontal displacements of the apparent shoreline [27]. In this study, all satellite images were selected to correspond to the same or quasi the same high tide levels, based on tidal records. The high tide values for the acquisition dates ranged from 2.52 m to 2.87 m, resulting in a maximum tidal range of 0.35 m across the 33-year period. This relatively narrow range ensures that the HWL was extracted under consistently high tidal conditions, thereby minimizing positional discrepancies. Nevertheless, a residual uncertainty due to slight tidal phase mismatches was acknowledged in the overall shoreline positioning error budget.

2) Seasonal Variability Error (E_s): Seasonal shoreline shifts, especially on sandy beaches, can cause significant variation due to storm events or sediment transport. However, all selected Landsat scenes correspond to the summer season, when the shoreline tends to be more stable. Therefore, this source of error was considered negligible for the purposes of this analysis.

3) Digitizing Error (E_d): This error reflects the uncertainty introduced during manual digitization of the HWL from NDWI imagery. Following the recommendations of the USGS, a maximum digitizing uncertainty of ±7.5 m (i.e., half a Landsat pixel) was assumed for each shoreline.

4) Pixel Resolution Error (E_p): Landsat TM, ETM+, and OLI data used in this study all have a 30 m spatial resolution, and no coarser data were included. Thus, pixel-related uncertainty was considered homogeneous across the dataset and incorporated within the digitizing error. No additional error from resolution discrepancy was included.

5) Georeferencing / Rectification Error (E_r): All Landsat Level-2 products used are already ortho-rectified and projected in UTM Zone 29N / WGS84. The standard geometric accuracy for these products is typically within ±7.5 m (USGS). This value was adopted as the rectification error for each shoreline.

The total positional uncertainty (U_t) for each shoreline was calculated using the root sum of squares (RSS) method, combining all individual sources of error:

$$U_t = \sqrt{E_s^2 + E_t^2 + E_d^2 + E_p^2} + E_r^2 \quad (2)$$

where: E_s: Seasonal error; E_t: Tidal error; E_d: Digitizing error; E_p: Pixel error; E_r: Rectification error.

To assess the uncertainty of shoreline, change rates over time, an annualized uncertainty () was derived using the following formula:

$$U_a = \pm \frac{\sqrt{\sum_{i=1}^{n} U_{ti}^2}}{T} \quad (3)$$

where U_t represents the total positional uncertainty of each shoreline and is the time span (in years) between the earliest and latest shoreline positions. This allowed for the expression of a confidence interval around the computed change rates in meters per year. The resulting U_t values were then integrated into DSAS v5.1 in ArcGIS 10.4 as weights to refine the Linear Regression Rate (LRR) and End Point Rate (EPR) calculations.

3. Results

Spatiotemporal Dynamics of Shoreline Change (1990–2023).

The shoreline evolution analysis over the 33-year period (1990–2023), based on 2,986 transects covering approximately 150.8 km of coastline, reveals significant spatial disparities in erosion and accretion processes. Despite a general trend toward net accretion, certain areas experienced substantial land loss.

The most affected zones in terms of net erosion are: Zone 4, which recorded the largest eroded area with 30,928 m^2 lost, Zone 1, with 17,791 m^2, and Zone 3, with 3,763 m^2.

Together, these losses amount to a total of 58,232 m^2 of land area eroded between 1990 and 2023, underscoring the presence of localised erosional hotspots within a generally accreting coastal system. The distribution of transects and shoreline length further reflects the relative weight of each sector in the analysis: Zone 4 encompasses the largest linear stretch (64.4 km) and the highest number of transects (1,261), followed by Zone 1 (33.6 km; 676 transects) and Zone 2 (23.9 km; 468 transects). These metrics ensured consistent spatial coverage and analytical resolution throughout the study area.

3.1. Shoreline Change Based on Linear Regression Rate (LRR)

The Linear Regression Rate (LRR) calculates the average trend of the shoreline position (**Figure 4**) over the entire study period by fitting a linear regression line to successive shoreline positions.

The LRR analysis across the whole study area indicates an average shoreline advancement of +0.37 m/year, reflecting an overall accretional dynamic.

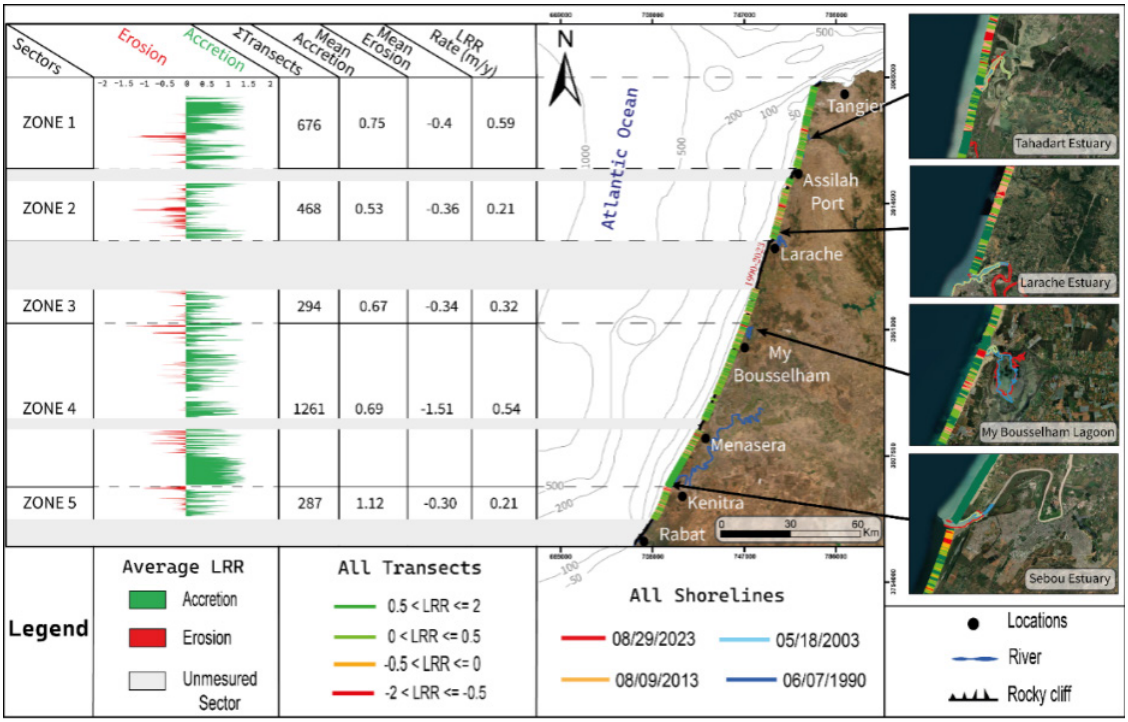

Figure 4. Shoreline evolution between 1990 and 2023 carried out by LRR statistical method.

Zone 1 shows the highest average accretion rate, at +0.59 m/year, reaching up to +2.4 m/year locally, but also exhibiting localized erosion areas with rates down to –3.49 m/year.

Zone 4 follows with +0.54 m/year, while Zones 2 and 5 present lower values (+0.21 to +0.15 m/year), indicating a more unstable sedimentary dynamic. Regarding the distribution of transects based on the LRR classification: i) 20% of transects show erosion, ii) 45% show accretion, iii) 36% show relative stability.

3.2. Shoreline Change Based on End Point Rate (EPR)

The End Point Rate (EPR) measures the average linear change between two extreme dates in the time series (**Figure 5**).

The average change rate measured by the EPR is slightly lower than that of the LRR, at +0.31 m/year for the overall study area. Zone 1 also records the highest average accretion (+0.53 m/year), followed by Zone 4 with +0.48 m/year. Zones 2 and 5 show lower trends, sometimes even negative, with rates around +0.15 m/year. Regarding the EPR classification: i) 23% of transects show erosion, ii) 42% show accretion, iii) 35% show stability.

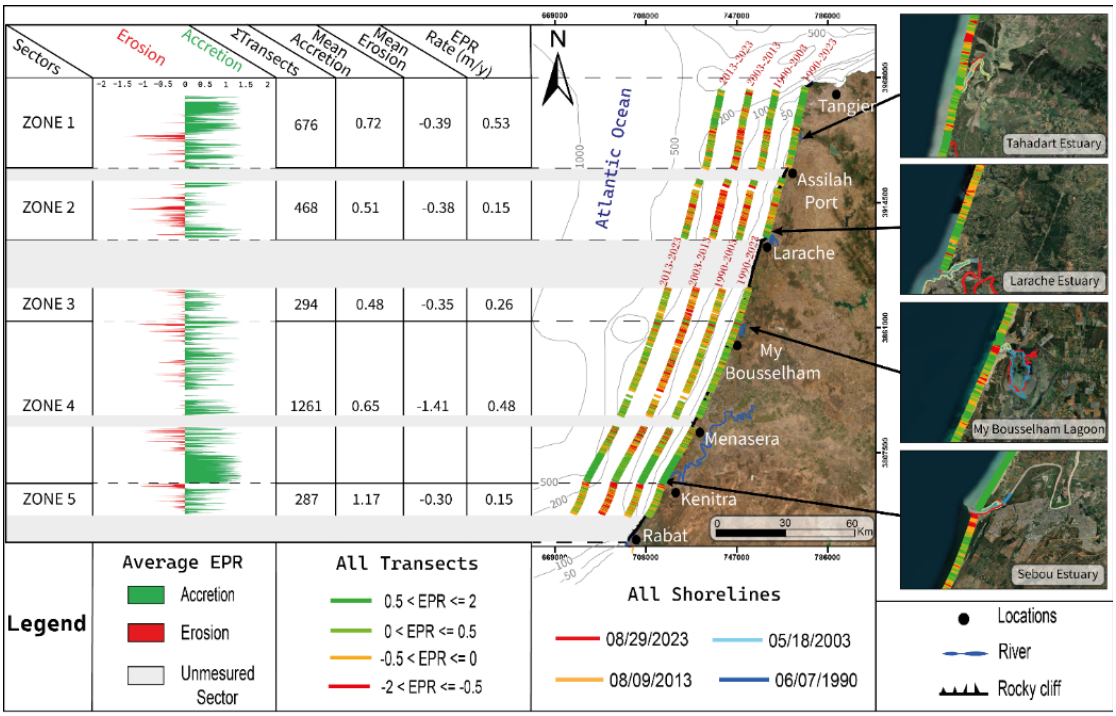

Figure 5. Shoreline evolution by periods carried out by EPR statistical method.

3.3.Comparison Between Linear Regression Rate (LRR) and End Point Rate (EPR)

Both the Linear Regression Rate (LRR) and End Point Rate (EPR) are widely used statistical methods for quantifying shoreline change, yet they differ in their approach and sensitivity. LRR estimates the average rate of shoreline change by fitting a least-squares regression line through all available shoreline positions over the entire study period. This method provides a robust and smooth trend that minimizes the influence of short-term fluctuations or anomalies, offering a comprehensive view of long-term coastal dynamics. In contrast, EPR calculates the rate of change based solely on the difference between two shoreline positions at the beginning and the end of the observation period. While simpler and computationally less demanding, EPR can be more sensitive to outliers or temporary shoreline positions, potentially exaggerating short-term variations.

In this study, LRR generally yielded slightly high-

er average accretion rates (+0.37 m/year) compared to EPR (+0.31 m/year), reflecting its smoothing effect over multiple data points. Both methods consistently identified Zone 1 as exhibiting the strongest accretion and Zones 2 and 5 as areas with weaker or unstable sediment dynamics.

Furthermore, the classification of transects by LRR and EPR showed comparable distributions of erosion, accretion, and stability, although EPR tended to detect a marginally higher percentage of erosional transects (23% vs. 20%). Overall, using both methods in tandem enhances confidence in the shoreline change assessment, with LRR providing a robust long-term trend and EPR offering a straightforward measure of net change between two key dates.

3.4. Temporal Evolution by Periods

The evolution of the shoreline over three distinct periods (1990–2003, 2003–2013, and 2013–2023) highlights notable variations in erosion and accretion trends (**Figure 4, Figure 5 and Table 3**).

Table 3. Statistics of LRR and EPR between 1990 and 2023 with a confidence interval of 99.9%.

Sectors		Zone 1	Zone 2	Zone 3	Zone 4	Zone 5	Σ Zones
Total of Transects		676	468	294	1261	287	2986
Length (m)		33567	23957	14472	64434	14381	150811
Total Area eroded 1990–2023 (m^2)		17791	3594	3763	30928	2157	58232
LRR	Mean Shoreline Change	0.59	0.21	0.32	0.54	0.21	0,37
	Max Shoreline Change	2.4	1.04	1.12	2.35	1.39	2.4
	Min Shoreline Change	–3.49	–2.33	–1.54	–1.04	–1.33	–3.49
	Total Erosional Transects	88	166	67	188	85	594
	Total Accretional Transects	379	134	111	658	77	1359
	Total Stable Transects	209	168	116	415	125	1033
	Erosion Transects (%)	13	35	23	15	30	20
	Accretion Transects (%)	56	36	38	52	27	45
	Stable Transects (%)	31	61	39	33	43	36
EPR	Mean Shoreline Change (m/y)	0,53	0.15	0.26	0.48	0.15	0,31
	Max Shoreline Change (m/y)	2.32	1.14	1.22	2.4	1.37	2.4
	Min Shoreline Change (m/y)	–3.4	–2.2	–1.4	–1.06	–1.4	–3.4
	Total Erosional Transects	105	183	76	219	105	688
	Total Accretional Transects	358	118	97	610	64	1247
	Total Stable Transects	213	167	121	432	118	1051
	Erosion Transects (%)	16	39	26	18	37	23
	Accretion Transects (%)	53	25	33	48	22	42
	Stable Transects (%)	31	36	41	34	41	35
Mean change 1990–2003		–0.23	–0.14	–0.03	0.18	–0.14	0.02
Mean change 2003–2013		–0.07	–0.45	–0.35	–0.13	–0.46	–0.29
Mean change 2013–2023		0.36	–0.02	0.10	0.31	–0.02	0.15

1990–2003: During this period, a general retreat of the shoreline is observed, with an average negative change of –0.23 m in Zone 1, –0.14 m in Zone 2, and -0.03 m in Zone 3. However, Zone 4 shows slight accretion (+0.18 m), while Zone 5 remains stable (–0.14 m). This period coincides with the construction of several upstream dams on major rivers, including Ibn Battouta (1977), Oued El Makhazine (1979), 9 Avril (1995), and El Wahda (1996), significantly reducing sediment supply to river mouths.

2003–2013: The trend slightly reverses, with an intensification of erosion in certain areas. Average rates become more negative, particularly in Zone 2 (–0.45 m) and Zone 5 (–0.46 m), confirming the growing impact of reduced sediment supply and sea-level rise. Zone 3 also exhibits slight retreat (–0.35 m), while Zone 4, previously accreting, begins to show minor retreat (–0.13 m).

2013–2023: The last decade is characterized by a general trend of stabilization and accretion in certain zones. The average change turns positive in Zone 1 (+0.36 m), Zone 3 (+0.10 m), and Zone 4 (+0.31 m), indicating potential recovery dynamics in these sectors. However, Zones 2 and 5 remain stable or slightly negative (–0.02 m), suggesting persistent erosional pressures.

The analysis of shoreline evolution for Moulay Bouslham, Tahadart, and Larache. These sites were selected due to their ecological and economic importance, as well as their vulnerability to erosion and accretion processes. These coastlines host sensitive ecosystems, support significant economic activities, and are subject to complex coastal dynamics influenced by both natural and anthropogenic factors. Shoreline evolution across these four areas exhibits contrasting trends (**Figure 4**, **Figure 5**):

a) Moulay Bousselham Lagoon

Located in the northern part of the study area and listed as a RAMSAR site, Moulay Bousselham displays strong shoreline variability: The northern shore shows a net accretion of +3.23 m/year, likely driven by sediment inputs from littoral drift and wave refraction effects. In contrast, the southern shore experiences active erosion, averaging –0.99 m/year.

A key observation is the significant morphological evolution of the lagoon inlet, which has recently narrowed to just 30 meters, signaling intense sedimentation and channel instability. These changes raise concerns for lagoon hydrodynamics, ecosystem resilience, and navigation.

b) Tahaddart-Gharifa Estuary

The Tahaddart sector is marked by a dominant trend of shoreline retreat, with an average erosion rate of −1.7 m/year. The erosion is most intense in the northern part, which has triggered a progressive southward migration of the littoral spit.

This geomorphic change has also shifted the mouths of the Tahaddart and Gharifa estuaries, influenced by strong net littoral drift and a deficit in sediment supply. The sector remains highly vulnerable, with ongoing modifications to estuarine channels and habitats.

c) Larache Coastline

Larache exhibits a moderate yet sustained erosion, with the shoreline retreating at −0.12 m/year on average. This evolution appears to result from: Sea-level rise, inducing chronic erosion on beach faces, Urban expansion and artificialization of the coastal strip, And reduced sediment inputs from the Loukkos River due to dam regulation and channelization. The sector presents high risks for coastal infrastructure, requiring integrated management strategies to mitigate erosion.

d) Kénitra – Sebou Delta (Mehdia, Sidi Boughaba, Chlihat)

The Kénitra coastline is characterized by spatially contrasted trends: Chlihat shows strong accretion at +4.7 m/year, mainly due to the northern accumulation effect induced by the 500 m-long jetties at the Sebou estuary mouth. Mehdia and Sidi Boughaba, situated south of the jetties, undergo severe erosion, with average retreat rates of −3.2 m/year and −1.97 m/year, respectively.

4. Discussion

The evolution of the shoreline observed between 1990 and 2023 in the study area highlights the complex and intertwined influences of natural dynamics, an-

thropogenic pressures, and climate-related factors. The spatial heterogeneity of erosion and accretion patterns across the five delineated zones is a direct reflection of varying coastal processes, modified sediment budgets, and episodic extreme events.

The results show that the northernmost sector (Zone 1) experienced the most significant accretion, with an average linear regression rate (LRR) of +0.59 m and a maximum shoreline advance of +2.4 m, while sectors such as Zone 2 and Zone 5 display more pronounced erosion tendencies, both showing lower mean change values (approximately +0.21 m LRR) and a higher proportion of erosional transects (35–39%). These patterns align with the known sediment transport regime in the area, primarily driven by dominant wave energy and littoral drift from north to south. In the Tahaddart region, for example, erosion reaches a critical rate of −1.7 m/year, a dynamic confirmed by El Habti [28], who documented widespread shoreline retreat over 87% between 1972 and 2019. These findings resonate with the sediment flux asymmetry generated by coastal morphology and wave refraction effects, which focus energy and sediment displacement onto the northern portion of the spit, gradually shifting it southward.

Moulay Bousselham illustrates a contrasting case of morphodynamic imbalance, where the northern beach sector accretes rapidly at +3.23 m/year, while the southern sector undergoes sustained erosion at −0.99 m/year. Our results echo the conclusions of Belrhaba et al., [28], who attribute this duality to the interaction between local hydrodynamics and regional climatic oscillations such as the Western European Pressure Anomaly (WEPA), influencing wave incidence angles and sediment deposition.

The Sebou Kénitra area reveals another compelling example of human-induced imbalance. Our study confirms a sharp spatial differentiation in shoreline trends, with intense accretion recorded at Chlihat (+4.7 m/year) on the northern side of the river mouth and severe erosion at Mehdia and Sidi Boughaba (−3.2 and −1.97 m/year, respectively) on the southern side. These dynamics are consistent with the morphosedimentary impact of the parallel jetties constructed at the estuary mouth. As shown by Hakkou et al., [24] and further supported by El Mrini et al., [29], these structures trap northward-moving sediments, preventing natural redistribution and thus amplifying downdrift erosion.

Beyond the natural forcing agents, anthropogenic activities have played a fundamental role in disrupting the coastal sediment equilibrium. Sand extraction, notably in Moulay Bousselham and Larache, has directly contributed to the retreat of dunes and beach systems, a phenomenon already demonstrated by Snoussi et al., [30] who highlighted the irreversible degradation caused by uncontrolled mining along Morocco's Atlantic beaches. In parallel, rapid urban expansion and the conversion of coastal lands for agricultural and tourism infrastructure particularly visible in the Tahaddart plain and the southern sectors of Larache have reduced the natural capacity of these environments to buffer wave energy, leading to increased exposure and retreat.

Furthermore, dam construction on upstream river systems has significantly altered sediment delivery to the coastal zone. Dams such as Ibn Battouta (1977), Oued El Makhazine (1979), and El Wahda (1996) have collectively reduced the annual sediment discharge of rivers like the Loukkos and Sebou by nearly 74%, from an estimated 34 million tonnes to just 8.8 million tonnes between 1996 and 1998 [31]. his sediment starvation directly translates into a long-term erosional deficit along the downstream beaches. Comparable situations have been documented globally, notably in the Mekong Delta [32] and in several Mediterranean deltas [33], where upstream damming combined with coastal development has accelerated shoreline retreat.

Climatic factors, particularly sea-level rise (SLR) and extreme storm events, further compound the vulnerability of this sandy coastline. Our observations align with broader global trends described by Vousdoukas et al. [34], who demonstrated that sandy coastlines will be among the first to retreat under the effects of SLR and increased storm frequency. This regional vulnerability is further confirmed by Aangri et al. [3,9], whose study on the Moroccan Atlantic coast showed that rising sea levels significantly accelerate shoreline retreat, especially in areas with low geomorphological resilience. In our study area, the major storm events of

2014 and 2017 support this assertion: the 2014 storm, with waves exceeding 7 meters, caused a retreat of more than 2 meters in Zone 2, while the 2017 storm reinforced ongoing erosion in Zone 5. These cumulative impacts emphasize the necessity of incorporating high energy episodic events into shoreline trend analysis, an often-overlooked dimension in conventional linear modeling approaches.

Moulay Bousselham, with its RAMSAR-listed lagoon, provides a particularly illustrative case of climate vulnerability. The progressive narrowing of the lagoon inlet from several hundred meters to only 30 m today signals intense sedimentation processes likely linked to both SLR and storm overwash. Similar dynamics have been documented in tidal inlets worldwide, such as in the Wadden Sea [35] and the Louisiana coast [36], where inlet morphology and function have been shown to respond sensitively to sea-level fluctuations and sediment supply constraints.

While the methodological approach used in this study based on multi-decadal Landsat imagery, high-water line (HWL) detection, and transect-based analysis via DSAS v5.1 ensures spatial and temporal consistency, it remains subject to known uncertainties. Despite the correction of geometric and radiometric biases, the spatial resolution of 30 meters and minor mismatches in tide levels introduce a positional uncertainty (Ut) of ±11.7 m. However, by integrating these uncertainties as weights in the calculation of LRR and EPR, our results remain robust and statistically reliable. Similar methodological frameworks have been adopted in studies across the Pacific [27,34] and in recent assessments of European coasts [34], confirming the relevance of our approach.

In light of these findings, urgent coastal management interventions are recommended. Limiting sand mining and implementing sediment bypassing systems at river mouths such as the Sebou estuary would mitigate the negative effects of sediment starvation. Similarly, restoring coastal dunes and wetland systems, can offer natural protection against wave impact and erosion. In some critical areas, adaptive engineering solutions like beach nourishment and vegetated revetments could be employed to stabilize vulnerable sectors.

Finally, future studies should build on this foundation by integrating higher resolution satellite data (e.g., Sentinel-2, Pleiades), in situ topographic monitoring (e.g., GPS and UAV surveys), and dynamic modeling of shoreline response under different sea-level and climate scenarios. A transdisciplinary framework combining remote sensing, hydrodynamic modeling, socio-economic assessments, and local knowledge will be essential to support the design of sustainable and resilient coastal management strategies across Morocco's Atlantic coast and beyond.

5. Conclusions

This study provides a comprehensive and long-term assessment of shoreline evolution along a critical stretch of the Moroccan Atlantic coast, covering a 33-year period from 1990 to 2023. Through a rigorous and reproducible geospatial methodology, based on multi-temporal Landsat imagery, High Water Line (HWL) shoreline proxies, and the Digital Shoreline Analysis System (DSAS v5.1), we were able to detect, quantify, and interpret the complex patterns of coastal change at both regional and local scales.

The methodological framework applied combining radiometric and geometric corrections, NDWI based shoreline extraction, visual verification, and statistically weighted linear trend analyses (LRR and EPR) proved both robust and adaptable to the characteristics of the study area. By harmonizing tide stages and minimizing sources of positional uncertainty, we ensured a reliable reconstruction of shoreline dynamics over multiple decades. The integration of DSAS allowed us to apply standardized transects and evaluate spatial variability with precision, while the uncertainty quantification added scientific rigor to our interpretations.

The results reveal a mosaic of shoreline behaviors: while some zones (such as Zone 1 and parts of Zone 4) exhibited consistent accretion, others (like Zones 2 and 5) were marked by persistent or episodic erosion. The highest net accretion was observed in the northern Moulay Bousselham area (+3.23 m/year), while the most severe erosion occurred in parts of Tahaddart (−1.7 m/year). These spatial differences

highlight the interplay between hydrodynamic forces, sediment transport regimes, human interventions (e.g., dams, jetties, urbanization), and climate variability, particularly the effects of sea-level rise and storm events. Our findings strongly align with international literature [15,34,36] and are further corroborated by regional studies [3,11,19,22].

The discussion underscores that no single factor can explain the observed patterns; rather, it is the convergence of natural, anthropogenic, and climatic influences that defines the current shoreline state. Moreover, extreme weather events often underestimated have proven decisive in reshaping coastal morphology over short timeframes, amplifying long-term trends. From a practical standpoint, the insights gained from this study are crucial for informing coastal management and adaptation strategies. The observed erosion in densely inhabited or ecologically sensitive areas (e.g., Mehdia, southern Moulay Bousselham) calls for immediate and integrated responses, including sediment management, dune rehabilitation, and the regulation of sand mining. The methodology developed here is transferable to other Moroccan or international coastal contexts, offering a replicable model for low-cost, large-scale shoreline monitoring using freely available remote sensing data.

Looking forward, future research should incorporate higher-resolution data (e.g., Sentinel-2, drone surveys), hydrodynamic modeling, and socio-economic vulnerability assessments. Furthermore, the integration of predictive tools under climate change scenarios will be essential for anticipating future shoreline trajectories and planning resilient coastal infrastructure. Ultimately, the synergy between earth observation, geomorphological analysis, and participatory coastal governance will be key to preserving the natural and socio-economic value of Morocco's Atlantic coast.

Author Contributions

Conceptualization, H.H. and M.H.; methodology, H.H.; software, H.H.; validation, H.H., M.H., S.S. and A.A.; formal analysis, H.H.; investigation, H.H.; resources, H.H.; data curation, H.H.; writing—original draft preparation, H.H.; writing—review and editing, A.A.; visualization, H.H.; supervision, M.H.; project administration, H.H.; funding acquisition, H.H. All authors have read and agreed to the published version of the manuscript.

Funding

This work received no external funding.

Institutional Review Board Statement

Not applicable.

Informed Consent Statement

Not applicable. This study did not involve human or animal subjects.

Data Availability Statement

The satellite imagery data used in this study (Landsat 5 TM, Landsat 7 ETM+, and Landsat 8 OLI) are publicly available and were obtained from the U.S. Geological Survey (USGS) EarthExplorer platform at https://earthexplorer.usgs.gov. All shoreline shapefiles generated and analyzed during this research are available from the corresponding author upon reasonable request. No proprietary or restricted data were used in this study.

Acknowledgments

We extend our sincere thanks to the U.S. Geological Survey (USGS) for providing open access to Landsat 5, 7, and 8 satellite imagery. These high-quality datasets were instrumental in supporting the temporal analysis of shoreline changes conducted in this study. We also acknowledge the sustained efforts of the USGS team in ensuring the continuity and availability of Earth observation data. Their contribution greatly facilitates scientific research in coastal monitoring and environmental assessment.

Conflicts of Interest

The authors declare no conflict of interest.

References

[1] Fletcher, C.H., Romine, B.M., Genz, A.S., et al., 2012. National assessment of shoreline change: Historical shoreline changes in the Hawaiian Islands. Available from: https://www.loc.gov/item/2023692538 (cited 11 May 2025).

[2] Duedall, I.W., Maul, G.A., 2005. Demography of Coastal Populations. In: Schwartz, M.L. (eds.). Encyclopedia of Coastal Science. Encyclopedia of Earth Science Series. Springer: Dordrecht, Netherlands. pp. 368–374.

[3] Aangri, A., Hakkou, M., Krien, Y., et al., 2022. Predicting shoreline change for the Agadir and Taghazout coasts (Morocco). Journal of Coastal Research. 38(5), 937–950. DOI: https://doi.org/10.2112/JCOASTRES-D-22-00006.1

[4] Aitali, R., Snoussi, M., Kasmi, S., 2020. Coastal development and risks of flooding in Morocco: The cases of Tahaddart and Saidia coasts. Journal of African Earth Sciences. 164, 103771. DOI: https://doi.org/10.1016/j.jafrearsci.2020.103771

[5] Gens, R., 2010. Remote sensing of coastlines: Detection, extraction, and monitoring. International Journal of Remote Sensing. 31, 1819–1836. DOI: https://doi.org/10.1080/01431160902926673

[6] Hereher, M.E., 2011. Mapping coastal erosion at the Nile Delta western promontory using Landsat imagery. Environmental Earth Sciences. 64(4), 1117–1125. DOI: https://doi.org/10.1007/s12665-011-0928-9

[7] IPCC, 2022. Summary for policymakers. In: Pörtner, H.-O., et al. (eds.). Climate Change 2022: Impacts, Adaptation and Vulnerability. Cambridge University Press: Cambridge, UK. pp. 3–34.

[8] Chtioui, T., Hakkou, M., Aangri, A., et al., 2024. The risk of marine submersion along the Ain Sbâa coastline with a maximum tide and pessimistic scenario of sea level rise (Atlantic, Morocco). https://doi.org/10.1007/978-3-031-47079-0_51 (cited 19 December 2024).

[9] Aangri, A., Hakkou, M., Krien, Y., et al., 2024. Risk assessment of marine flooding along the Agadir and Taghazout coasts (Moroccan Atlantic). Journal of Coastal Research. 40(1), 179–192. DOI: https://doi.org/10.2112/JCOASTRES-D-23-00033.1

[10] Gong, P., 2012. Remote sensing of environmental change over China: A review. Chinese Science Bulletin. 57(22), 2793–2801. DOI: https://doi.org/10.1007/s11434-012-5268-y

[11] Belrhaba, T., Hakkou, M., Rey, T., et al., 2024. Shoreline change and climatic variability along the Moulay Bousselham coast (Moroccan Atlantic). Journal of Coastal Research. 40(5), 860–874. DOI: https://doi.org/10.2112/JCOASTRES-D-23-00082.1

[12] Environmental Systems Research Institute (ESRI), 2018. Understanding raster georeferencing. Available from: https://www.esri.com/about/newsroom/wp-content/uploads/2018/07/Understanding-Raster-Georeferencing.pdf (cited 15 February 2025).

[13] Ekercin, S., 2007. Coastline change assessment at the Aegean Sea coasts in Turkey using multitemporal Landsat imagery. Journal of Coastal Research. 23(3), 691–698. DOI: https://doi.org/10.2112/04-0398.1

[14] Dyer, K.R., 2021. Response of estuaries to climate change. In: Eisma, D. (eds.). Climate Change: Impact on Coastal Habitation. CRC Press: Boca Raton, FL, USA. pp. 85–110.

[15] Kovalskyy, V., Roy, D.P., 2013. The global availability of Landsat 5 TM and Landsat 7 ETM+ land surface observations and implications for global 30 m Landsat data product generation. Remote Sensing of Environment. 130, 280–293. DOI: https://doi.org/10.1016/j.rse.2012.12.003

[16] Moore, J.L., 2000. Techniques de cartographie des rivages. Journal du Littoral Recherche. 16(1), 111–124.

[17] Alesheikh, A.A., Ghorbanali, A., Nouri, N., 2007. Coastline change detection using remote sensing. Journal of Coastal Research. 4, 61–66. DOI: https://doi.org/10.1007/BF03325962

[18] Snoussi, M., & LDK Consultants Engineers & Planners SA. (n.d.). EFH-MO-5: Contribution to the development of an Integrated Coastal Zone Management Plan for the Rabat-Salé-Kénitra Region. Task 1: Diagnostic analysis of the coastal zones of the Region. SWIM-H2020. http://www.abhatoo.net.ma/maalama-textuelle/developpement-durable/environnement/milieux-marins/ecosysteme-du-littoral/zones-cotieres/efh-mo-5-contribution-a-l-elaboration-d-un-plan-de-gestion-integree-pour-les-zones-cotieres-de-la-region-de-rabat-sale-kenitra-tache-1-diagnostic--des-zones-cotieres-de-la-region-de-rabat-sale-kenitra (cited 17 November 2020).

[19] Hakkou, M., Castelle, B., Benmohammadi, A., et al., 2011. Wave climate and morphosedimentary characteristics of the Kenitra–Bouknadel sandy

coast, Morocco. Environmental Earth Sciences. 64, 1729–1739. DOI: https://doi.org/10.1007/s12665-011-0977-0

[20] Klemas, V., 2011. Remote sensing techniques for studying coastal ecosystems: An overview. Journal of Coastal Research. 27(1), 2–17.

[21] Aangri, A., Hakkou, M., Krien, Y., et al., 2024. Mapping the shoreline evolution in response to sea level rise along Agadir Bay, Morocco: Geospatial and empirical approach. Available from: https://doi.org/10.1007/978-3-031-47079-0_68 (cited 24 November 2024).

[22] Chtioui, T., Hakkou, M., Aangri, A., et al., 2024. Storm's influence on long-term shoreline evolution along Casablanca-Mohammedia (Morocco). Regional Studies in Marine Science. 75, 103549. DOI: https://doi.org/10.1016/j.rsma.2024.103549

[23] Hakkou, M., Maanan, M., Belrhaba, T., et al., 2019. Assess and mapping the flooding hazards using geospatial tools and empirical models along Kenitra coast, Morocco. Ocean & Coastal Management. 169, 264–272. DOI: https://doi.org/10.1016/j.ocecoaman.2018.12.032

[24] Hakkou, M., Maanan, M., Belrhaba, T., et al., 2018. Multi-decadal assessment of shoreline changes using geospatial tools and automatic computation in Kenitra coast, Morocco. Ocean & Coastal Management. 163, 232–239. DOI: https://doi.org/10.1016/j.ocecoaman.2018.07.003

[25] Mitasova, H., Thaxton, C., Hofierka, J., McLaughlin, R., Moore, A., Mitas, L., 2004. Path sampling method for modeling overland water flow, sediment transport, and short-term terrain evolution in Open Source GIS. Developments in Water Science. 55, 1479–1490.

[26] Hapke, C.J., Himmelstoss, E.A., Kratzmann, M.G., et al., 2011. National assessment of shoreline change: Historical shoreline change along the New England and Mid-Atlantic coasts. U.S. Geological Survey Open-File Report 2010-1118.

[27] Fletcher, C.H., Mullane, R.A., Richmond, B.M., 1997. Beach Loss along Armored Shorelines on Oahu, Hawaiian Islands. Journal of Coastal Research. 13(1), 209–215. Available from: http://www.jstor.org/stable/4298607

[28] El Habti, M.Y., Zayoun, A., Salim, F.Z., et al., 2022. Shoreline change analysis along the Tahaddart coast (NW Morocco): A remote sensing and statistics-based approach. Journal of Coastal Research. 38(6), 1116–1127. DOI: https://doi.org/10.2112/JCOASTRES-D-22-00026.1

[29] El Mrini, A., Nachite, D., & Taaouati, M. (2008, January). Interactions physico-naturelles et socio-economique sur le littoral tetouanais (maroc nord occidental). In Actes du colloque international pluridisciplinaire Le littoral: subir, dire, agir-Lille, France.

[30] Snoussi, M., Ouchani, T., & Niazi, S. (2008). Vulnerability assessment of the impact of sea-level rise and flooding on the Moroccan coast: The case of the Mediterranean eastern zone. Estuarine, Coastal and Shelf Science, 77(2), 206–213. https://doi.org/10.1016/j.ecss.2007.09.024

[31] Snoussi, M., Haïda, S., Imassi, S., 2002. Effects of the construction of dams on the water and sediment fluxes of the Moulouya and the Sebou Rivers, Morocco. Regional Environmental Change. 3(1), 5–12. DOI: https://doi.org/10.1007/s10113-001-0035-7

[32] Syvitski, J.P.M., Kettner, A.J., Overeem, I., et al., 2009. Sinking deltas due to human activities. Nature Geoscience. 2(10), 681–686. DOI: https://doi.org/10.1038/ngeo629

[33] Anthony, E.J., Gaudio, S.D., Héquette, A., 2014. Coastal erosion in the Mediterranean region: A review of recent events and processes. Geological Society, London, Special Publications. 388(1), 121–137. DOI: https://doi.org/10.1144/SP388.5

[34] Vousdoukas, M.I., Ranasinghe, R., Mentaschi, L., et al., 2020. Sandy coastlines under threat of erosion. Nature Climate Change. 10(3), 215–222. DOI: https://doi.org/10.1038/s41558-020-0697-0

[35] Friedrichs, C.T., 2011. Tidal flat morphodynamics: A synthesis. In: Wolanski, E., McLusky, D. (eds.). Treatise on Estuarine and Coastal Science. Elsevier: Oxford, UK. pp. 137–170.

[36] Morton, R.A., Barras, J.A., 2011. Hurricane impacts on coastal wetlands: A half-century record of storm-generated features from southern Louisiana. Journal of Coastal Research. 27(6A), 27–43. DOI: https://doi.org/10.2112/JCOASTRES-D-10-00185.1